CNRS
Centre National de la Recherche Scientifique

NIKHEF
Nationaal instituut voor subatomaire fysica

INFN
Instituto Nazionale di Fisica Nucleare

Advanced Virgo Output Mode Cleaner: Optimization of the cavity parameters to minimize the thermo-refractive noise.

R. Gouaty, R. Bonnand, F. Marion, B. Mours, L. Rolland

VIR-0016A-13

January 29, 2013

Contents

1 Introduction

Polishing specifications for the OMC cavities have been presented in [1, 2]. Since the writing of these documents, it has been shown in [3] that the thermo-refractive noise of the OMC cavities is about 3 orders of magnitude larger than what was expected for the thermo-elastic noise. Such noise couples to the interferometer output port proportionally to the OMC length offset with respect to the cavity resonance. Therefore the thermo-refractive noise puts constraints on the OMC locking accuracy. An upper limit on the locking accuracy for the Virgo OMC was measured [1] at the level of $6 \times 10^{-12}\ m$. As shown in [3] and under the assumption of the OMC parameters presented in [1], the OMC locking accuracy for Advanced Virgo would have to be a factor 20 lower than this upper limit, in order to keep the OMC length noise a factor 10 or more below the Advanced Virgo nominal sensitivity, in the whole interferometer bandwidth (starting from 10 Hz). As it was discussed in [4] a significant improvement of the OMC locking accuracy is expected with respect to the previously measured upper limit. However, since the Advanced Virgo OMC locking accuracy is not yet quantified [2], it is relevant to optimize the design of the OMC cavities in order to relax a bit the constraints on their locking accuracy. The goal of this note is to discuss some possible optimization of the OMC parameters in order to reduce the impact of the thermo-refractive noise.

As shown in [5] the amplitude spectrum of the thermo-refractive noise is inversely proportional to the square of the beam waist in the OMC cavity. This means that by increasing the cavity radius of curvature (and consequently the waist) one can reduce the thermo-refractive noise. An optimization of the OMC radius of curvature is presented in Section 2.

Another parameter to be optimized is the OMC finesse, as the coupling of the length noise is proportional to the square of the finesse. A possible reduction of the finesse is discussed in Section 3.

The benefits of these parameter optimizations for the OMC thermo-refractive noise will be shown in Section 4.

2 Optimization of the OMC radius of curvature

Aside the value of the radius of curvature (RoC) that is discussed here, the other OMC parameters considered in this section are the same as the ones presented in Appendix A in [1]. They

[1] Virgo logbook 28709

[2] A correct estimate of the Advanced Virgo OMC locking accuracy first requires a completed design of the OMC control system (which is still on-going at present time) and also rely on experimental tests to be performed in 2013 with the Advanced Virgo OMC cavities

are summarized in Tab.1 with the allowed polishing error bars[3]. The corresponding technical drawing (with a new value for the RoC that will be discussed later) is shown in Fig.1. The geometrical length and the optical length are related to the parameters L and θ used in Fig.1 as follows:

$$L_{geo} = \frac{L}{2}\left(1 + \frac{1}{cos(2\theta)}\right) \tag{1}$$

$$L_{opt} = 2nL_{geo} \tag{2}$$

where n is the refraction index of fused silica at 1064 nm: $n = 1.44963$.
The value of the waist w_0 is related to the radius of curvature of the spherical surface (ρ) according to the relation:

$$w_0 = \sqrt{\frac{\lambda}{n\pi}\sqrt{2L_{geo}(\rho - 2L_{geo})}} \tag{3}$$

Finesse	L_{opt} (mm)	L_{geo} (mm)	Inc. angle (°)	Clear Aperture Diameter (mm)
210	179.8 ± 0.6	62.0 ± 0.2	6.00 ± 0.02	8

Table 1: *Assumptions on OMC parameters considered for the discussion on the RoC optimization. These values correspond to the design presented in Appendix A of [1] and in [2]. L_{geo} refers to the cavity geometrical length and L_{opt} to the optical length ($L_{opt} = 2nL_{geo}$).*

In [1] (Appendix A) and [2], a nominal radius of curvature equal to 789.2 mm had been chosen in order to minimize the amount of power transmitted by the OMC in the high order modes (HOM) of the carrier and the side bands. As the residual power in the HOM was about an order of magnitude lower than the specifications (see [1], Table 8), it is possible to select a larger RoC value that still satisfies the requirements on HOM filtering, as it is discussed in the following. In section 2.1 we will first present the limitation on the maximum RoC value imposed by the surface tilt errors and the constraints on the clear aperture. In section 2.2 we will discuss a possible trade-off between the maximization of the cavity waist and the filtering of high order modes.

2.1 Limitation on the maximum RoC due to surface tilt errors

In order to reduce the thermo-refractive noise of the OMC one should maximize the waist of the cavity (by increasing the RoC of the spherical surface). A limitation on the maximum RoC value is fixed by the available clear aperture on the OMC surfaces ($\Phi = 8\ mm$) and the allowed manufacturing error bar for the tilt angle of each surface ($\delta\theta = \pm 0.02°$). The impact of an error

[3]For the incidence angle of the beam resonating inside the cavity the allowed error bar considered in [1] was $\pm 0.03°$. However, after further discussion the polishing company has agreed to aim at an error bar of $\pm 0.02°$ as best effort. Thus this latest value is assumed in this note.

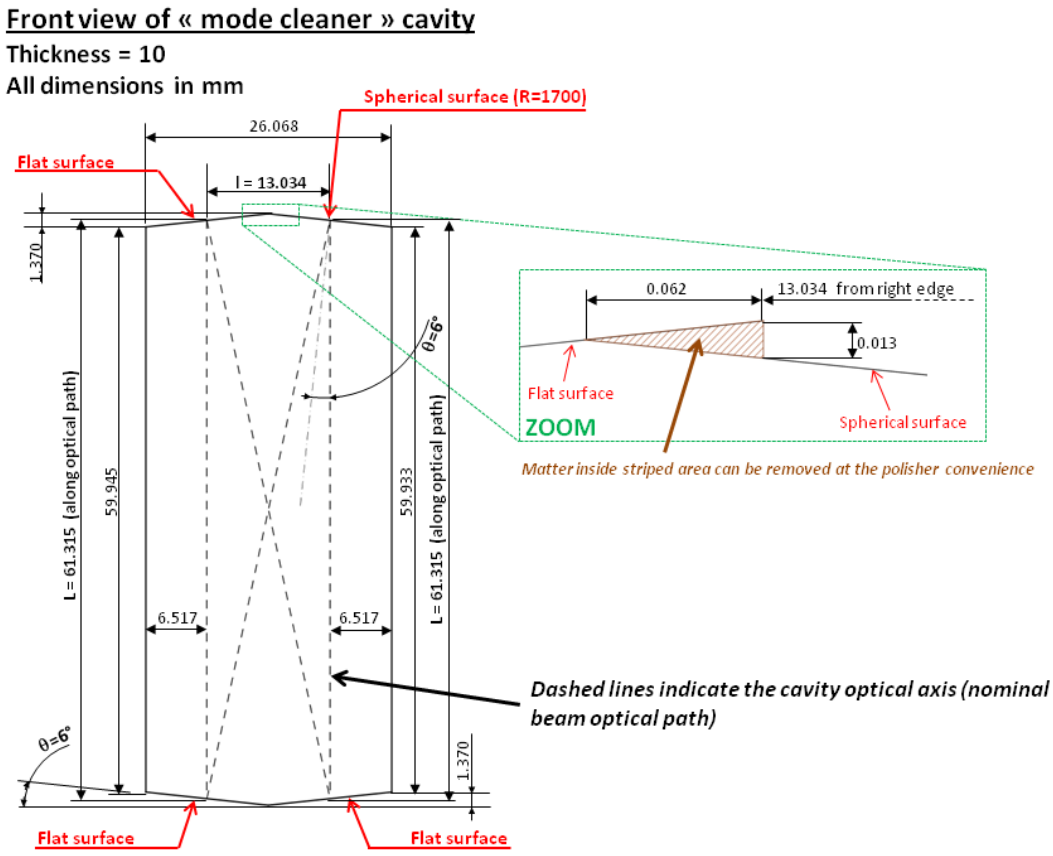

Figure 1: Technical drawing for the Advanced Virgo OMC, assuming a radius of curvature of 1700 mm.

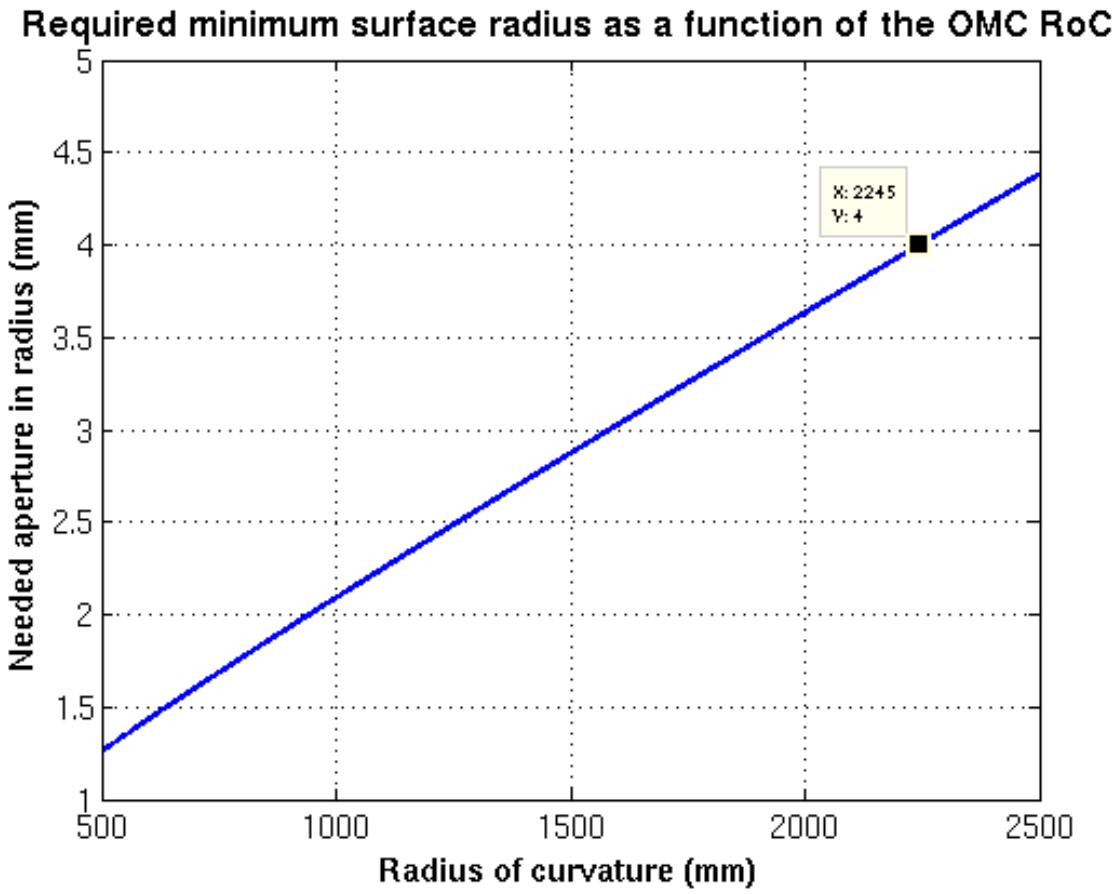

Figure 2: Needed surface aperture as a function of the OMC radius of curvature, assuming an absolute angular error of 0.02° on each surface for the worst tilt configuration.

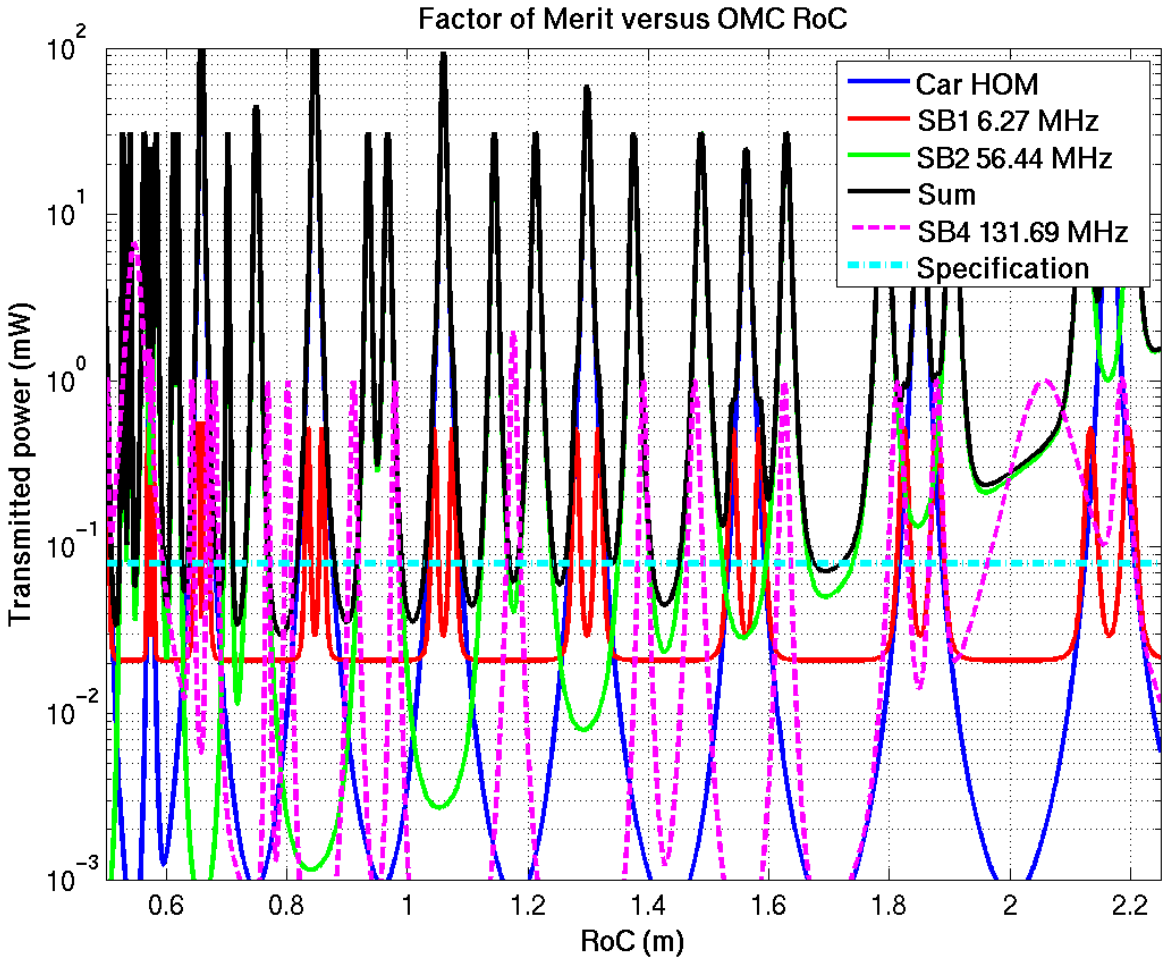

Figure 3: Sum of side bands and high order modes expected in transmission of the OMC as a function of the OMC RoC. The black curve stands for the total factor of merit (FoM) that includes the sum of all carrier high order modes, and all 6.27 MHz and 56.44 MHz side band components. The blue curve corresponds to the carrier FoM (sum of carrier HOMs). The red curve (respectively green) stands for the contribution of the 6.27 MHz (respectively 56.44 MHz) side band. A FoM has also been calculated for the 131 MHz side band and is shown as the magenta dotted curve. The specifications provided by ISC [7] on the acceptable residual power in each frequency component is shown by the horizontal cyan dash-dot line.

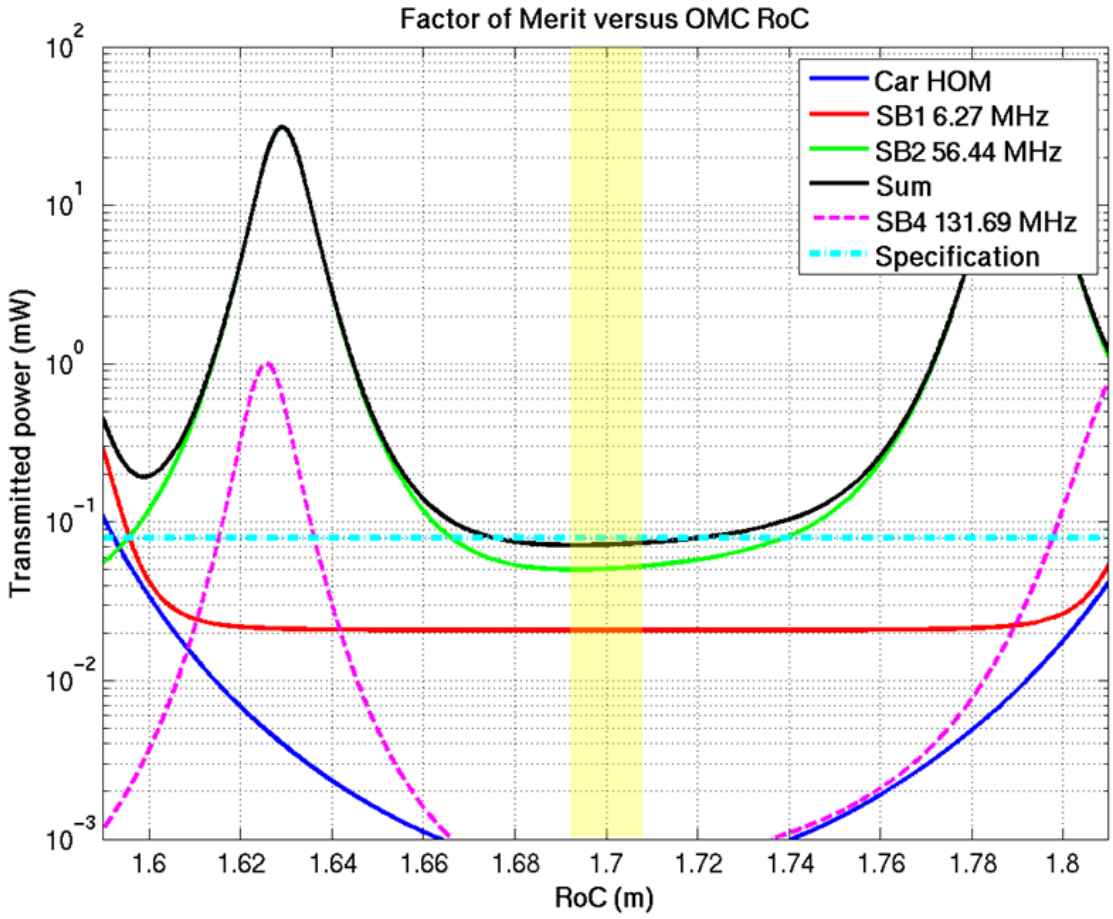

Figure 4: Sum of side bands and high order modes expected in transmission of the OMC as a function of the OMC RoC: ZOOM. The yellow shadowed area represents the possible location of the RoC, assuming a nominal value of 1700 mm with an allowed error bar of ± 8 mm (as proposed by the polishing company).

on the cavity surface tilt has been deeply studied in [6]: in presence of a static misalignment of the OMC surfaces, the optical axes of the cavity are slightly misaligned and, consequently, the beam is miscentered with respect to the OMC surfaces. The study presented in [6] has allowed to quantify this miscentering (d), which, under the most pessimistic configuration for which the angular errors on the four surfaces are adding up, can be approximated by:

$$d \approx 4\frac{\delta\theta}{\rho} \tag{4}$$

By requesting that the miscentered beam stays within the surface clear aperture (with a margin of $2.5w_0$ in order to avoid clipping), one obtain the following condition on the requested clear aperture radius (R_{CA}):

$$R_{CA} \geq 4\frac{\delta\theta}{\rho} + 2.5 \times \sqrt{\frac{\lambda}{n\pi}\sqrt{2L_{geo}\left(\rho - 2L_{geo}\right)}} \tag{5}$$

The needed clear aperture radius as a function of the cavity radius of curvature (for the most pessimistic configuration of surface tilts, assuming an absolute angular error of 0.02° on each surface) is shown in Fig.2. As the clear aperture radius that has been requested to the polishing company (cf. Tab.1) is 4 mm, one can deduce from Fig.2 that the cavity radius of curvature must be kept smaller than 2245 mm.

2.2 Choice of a new RoC

In order to find the best trade-off between the maximization of the cavity waist and a sufficiently good filtering of the side bands and high order modes, one can use the same factor of merit as the one defined in [1]. This factor of merit (FoM) corresponds to the sum of all high order modes and all side bands components (including the side bands TEM_{00}) that are expected in transmission of the second OMC cavity. As done in [1] the quantity FoM is evaluated by using the same assumptions on the HOM and SB power before the OMC as the ones presented in the Technical Design Report [7] (see Tab. 7.4 in the TDR).
The factor of merit expected for the Advanced Virgo Dual Recycling 125W configuration is plotted as a function of the OMC RoC (which is designed to be the same for both OMC cavities as explained in [1]) in Fig. 3 for RoC values ranging from 500 mm to 2250 mm (given the limitation on the maximum RoC value explained in section 2.1). One can deduce from this figure that the maximum RoC value compliant with the specifications provided by ISC (see the cyan dash-dot line in Fig. 3) is about 1700 mm. A zoom of the FoM around this RoC value is shown in Fig. 4. For such a RoC value, the polishing company proposes a manufacturing error bar of ± 8 mm. The possible location of the RoC given this error bar and assuming a nominal value at 1700 mm is represented by the yellow-shadowed area in Fig. 4. One can conclude that this RoC value and its error bar are compatible with the filtering requirements on the carrier and side bands.

2.3 Filtering performances with a RoC of 1700 mm and a finesse of 210

The transmission factors and the residual powers obtained after two mode cleaner cavities with a RoC of 1700 mm and the parameters presented in Tab. 1 have been estimated for each mode up to $m + n = 14$ (where m and n refer to the indexes of the TEM modes). Modes of higher order have such an extended spatial profile that they will not be accepted by the system aperture. For the HOM and SB power before the OMC the same assumptions are used as the ones made in the Technical Design Report [7] (see Tab. 7.4 in the TDR). The residual powers after the OMC cavities are shown in Tab. 2 for the carrier HOM, the side bands TEM_{00} and HOM at 6 MHz and 56 MHz.
One can observe that the total power estimated in the 6 MHz side band is about a factor 4 below the specifications and is dominated by the TEM_{00}, while the total power estimated in the 56 MHz side band is about a factor 1.6 below the specifications and is dominated by the high order modes. Actually the dominating high order mode for the 56 MHz side band is the mode of order 1, which contains about 44.4 mW in transmission of the OMC cavities, assuming that the power in this mode before the OMC cavities is 400 mW. Such assumption was considered in [7] and in [1] but is arbitrary as no simulation result concerning the HOM of the 56 MHz side band induced by misalignments is available yet. Nevertheless the relevancy of this assumption can be challenged as it is expected to be well overestimated. Indeed this assumption implies that the 1^{st} order mode of the 56 MHz side band would be 2.5 times larger than the power in its TEM_{00}, which is expected to be about 160 mW at the dark fringe. Contrary to the carrier TEM_{00} which is tuned at the dark fringe and is not resonant in the signal recycling cavity, the 56 mHz side band TEM_{00} is partially transmitted towards the interferometer output port through the Schnupp asymmetry and is resonant in the signal recycling cavity. Therefore the power of the 56 MHz side band 1^{st} order mode transmitted at the dark fringe cannot be larger than the power in the TEM_{00} but should rather be a fraction of it. To conclude, the powers reported in Tab. 2 for the 56 MHz side band high order modes are overestimated and the dominating contribution to the residual transmitted power should come from the 6 MHz side band TEM_{00} which is significantly below the specifications.

3 Optimization of the OMC finesse

In this section, a possible reduction of the OMC finesse is investigated in order to reduce the coupling of the OMC length noise which goes as the square of the finesse. The results that are discussed in the following have been obtained by considering the optical parameters presented in the Tab. 3 for the two OMC cavities. The radius of curvature is chosen to be 1700 mm, as a result of the optimization presented in section 2.

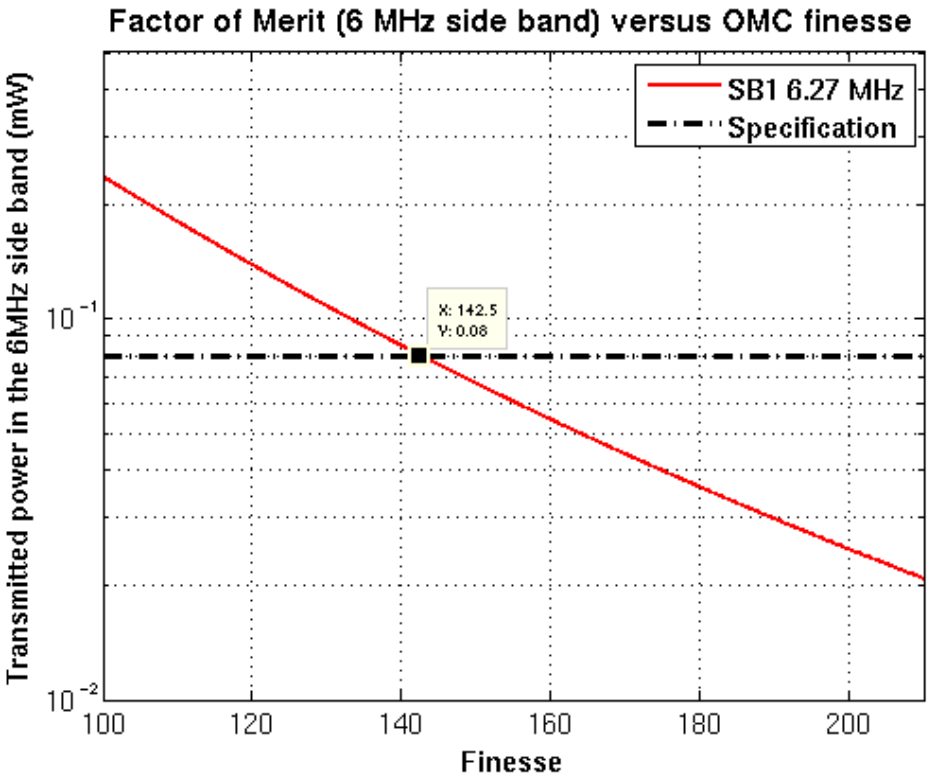

Figure 5: Sum of the TEM_{00} and high order modes for the 6 MHz side band expected in transmission of the OMC as a function of the finesse of the OMC cavities. The black dash-dot line indicates the specification for the dual recycling 125 W configuration.

Dual recycling 125W					
L_{geo} ρ	61.80 mm 1692 mm	61.80 mm 1708 mm	Nominal WP 62.00 mm 1700 mm	62.20 mm 1692 mm	62.20 mm 1708 mm
Carrier HOM Total	0.6μW	0.6μW	0.6μW	0.6μW	0.6μW
Carrier Specifications	$\leq 80\mu$W				
SB1 TEM_{00}	21.0μW	21.0μW	20.8μW	20.5μW	20.5μW
SB1 HOM	0.03μW	0.03μW	0.03μW	0.03μW	0.03μW
SB1 Total	21.0μW	21.0μW	20.8μW	20.6μW	20.5μW
SB1 Specifications	$\leq 80\ \mu$W				
SB2 TEM_{00}	0.3 μW	0.3 μW	0.3 μW	0.2 μW	0.2μW
SB2 HOM	48.5 μW	52.6μW	50.5μW	52.1μW	52.8μW
SB2 Total	48.7 μW	52.8μW	50.7μW	52.3μW	53.0μW
SB2 Specifications	$\leq 80\ \mu$W				

Table 2: *Transmission of the carrier HOM and side bands after the two OMC cavities in the SR 125W configuration with a finesse F=210. The transmitted power is computed for five different working points (WP): the nominal WP ($\rho = 1700$ mm, $l_{geo} = 62.0$ mm), and four other WPs corresponding to the extrema of the allowed manufacturing error bars ($l_{geo} = 62.0 \pm 0.2$ mm and $\rho = 1700 \pm 8$ mm). SB1 refers to the side-band at 6.27 MHz and SDB2 to the side-band at 56.44 MHz.*

3.1 Minimum finesse given ISC specifications on the 6 MHz side band filtering

As discussed in section 2.3 the assumption previously made for the power in the 1^{st} order mode of the 56 MHz side band before the OMC cavities is overestimated and not realistic. As there is no simulation result available for this mode, making a prediction seems quite difficult. Therefore, we will only consider the 6 MHz side band (whose TEM_{00} mode is expected to be

L_{opt} (mm)	L_{geo} (mm)	Radius of curvature of the convex surface (mm)
179.8 ± 0.6	62.0 ± 0.2	1700 ± 8

Table 3: *Assumptions on OMC parameters considered for the discussion on the finesse optimization. The radius of curvature of the spherical surface is chosen to be 1700 mm as a result of the optimization discussed in section 2. The other parameters correspond to the design presented in Appendix A of [1] and in [2]. L_{geo} refers to the cavity geometrical length and L_{opt} to the optical length ($L_{opt} = 2nL_{geo}$).*

the dominant contribution to the residual power transmitted by the second OMC cavity, aside the carrier TEM_{00} mode) for the optimization of the finesse. Once a finesse value has been selected, we will check which amount of power in the 56 MHz side band 1^{st} order mode can be accepted with this finesse to fit the specifications.

The power for the 6 MHz side band in transmission of the second OMC cavity obtained by summing up the TEM_{00} and all the high order modes is plotted as a function of the OMC finesse (supposed to be identical for the two cavities) in Fig. 5. This result is based on the assumptions previously made for the 6 MHz power before the OMC cavity (see Tab. 7.4 in [7]) which are reminded in Tab. 4. Fig. 5 shows that the minimum finesse value compliant with the specifications on the 6 MHz side band filtering set by ISC [7] is 143. This finesse will be considered in the following.

3.2 Filtering performances with a RoC of 1700 mm and a finesse of 143

Order $m+n$	0	1	2	3	4	5	6	7	8	9	10	11	...	14
Carrier (mW)	80	200	60	25	25	25	60	250	250	95	60	25	...	25
SB1 (mW)	2.5	6.3	1	1	1	1	1	1	1	1	1	1	...	1
SB2 (mW)	160	80	62	62	62	62	62	62	62	62	62	62	...	62

Table 4: *Assumptions on TEM_{00} and HOM power used to calculate the residual power in transmission of the two OMC cavities in the dual recycling configuration (125 W of injected power).*

Assuming a finesse equal to 143, one can evaluate the maximum acceptable power in the 1^{st} order mode of the 56 MHz side band before the OMC, by requesting that this power remains compliant with the specifications (transmitted side band $\leq 80\mu$W) and taking into account the allowed manufacturing error bars on the length ($\pm 200\mu m$) and radius of curvature ($\pm 8mm$). One finds that the power in the 1^{st} order mode of the side band can be as high as 80 mW which represents about half of the power expected in the 56 MHz side band TEM_{00}. Such limitation on the 56 MHz side band 1^{st} order mode power seems to be realistic, which confirms that the choice of a finesse equal to 143 is compatible with the requirements on the 56 MHz side band filtering.
In order to evaluate the residual power in the high order modes and side bands obtained in transmission of the second OMC cavity, one will now use the assumption on the power reaching the first OMC cavity that are summarized in Tab. 4. Apart for what concerns the 56 MHz side band 1^{st} order mode (for which we assume a maximum power of 80 mW as discussed above), all the other modes are assumed to be at the same level of power as what was considered in previous documents [7, 1]. The residual powers after the OMC cavities in the dual recycling

Dual recycling 125W					
L_{geo} ρ	61.80 mm 1692 mm	61.80 mm 1708 mm	Nominal WP 62.00 mm 1700 mm	62.20 mm 1692 mm	62.20 mm 1708 mm
Carrier HOM Total	2.7μW	2.9μW	2.7μW	3.0μW	2.7μW
Carrier Specifications	$\leq 80\mu$W				
SB1 TEM_{00}	79.9μW	79.9μW	79.0μW	78.2μW	78.2μW
SB1 HOM	0.1μW	0.1μW	0.1μW	0.1μW	0.1μW
SB1 Total	80.0μW	80.0μW	79.2μW	78.3μW	78.3μW
SB1 Specifications	$\leq 80\ \mu$W				
SB2 TEM_{00}	1.2μW	1.2μW	1.2μW	1.2μW	1.2μW
SB2 HOM	67.4μW	72.3μW	67.4μW	78.8μW	68.3μW
SB2 Total	68.5μW	73.5μW	68.6μW	79.9μW	69.4μW
SB2 Specifications	$\leq 80\ \mu$W				

Table 5: *Transmission of the carrier HOM and side bands after the two OMC cavities in the SR 125W configuration, with a finesse F=143. The transmitted power is computed for five different working points (WP): the nominal WP ($\rho = 1700$ mm, $l_{geo} = 62.0$ mm), and four other WPs corresponding to the extrema of the allowed manufacturing error bars ($l_{geo} = 62.0 \pm 0.2$ mm and $\rho = 1700 \pm 8$ mm). SB1 refers to the side-band at 6.27 MHz and SDB2 to the side-band at 56.44 MHz. The assumptions made on the power before the OMC cavities are given in Tab. 4.*

125 W configuration are shown in Tab. 5 for the carrier HOM, the side bands TEM_{00} and HOM at 6 MHz and 56 MHz. Again only modes of order up to $m+n = 14$ have been included in this computation, as higher order modes have such an extended spatial profile that they will not be accepted by the system aperture.
One can conclude from Tab. 5, that the specifications given by ISC[7] are satisfied with a finesse equal to 143, even at the margin of the allowed manufacturing error bars on the OMC length and radius of curvature.

4 Impact on the OMC thermo-refractive noise

As discussed in [5] and quoted in [3], the OMC thermo-refractive noise (δl_{tr}) can be evaluated using the following relation:

$$\delta l_{tr} \approx \frac{2\beta\sqrt{L_{rt}k_b}\kappa T}{DC}\frac{1}{\sqrt{\pi}\left(w/\sqrt{2}\right)^2 2\pi f} \tag{6}$$

The parameters used in the previous equation [3] are defined in Tab. 6. As discussed in [3] the length noise of the two OMC cavities couples to the interferometer sensitivity according to the

Parameter	Symbol	Value
Temperature dependence of refractive index	β	$-1.0 \times 10^{-5} K^{-1}$
Substrate density	D	$2200 kg/m^3$
Geometrical round-trip length	$L_{rt} = 4L_{geo}$	248 mm
Thermal conductivity	κ	$1.38 W m^{-1} K^{-1}$
Temperature	T	300 K
Specific heat	C	$746 J K^{-1} kg^{-1}$
Boltzmann constant	k_b	$1.38 \times 10^{-23} m^2 kg s^{-2} K^{-1}$
Beam width (approximated by cavity waist)	w	$259 \mu m$ for $\rho = 789.2$ mm $321 \mu m$ for $\rho = 1700$ mm

Table 6: *Parameters used for the evaluation of the thermo-refractive noise. The beam width (w) in the OMC cavity is approximated by the cavity waist, which is a conservative hypothesis.*

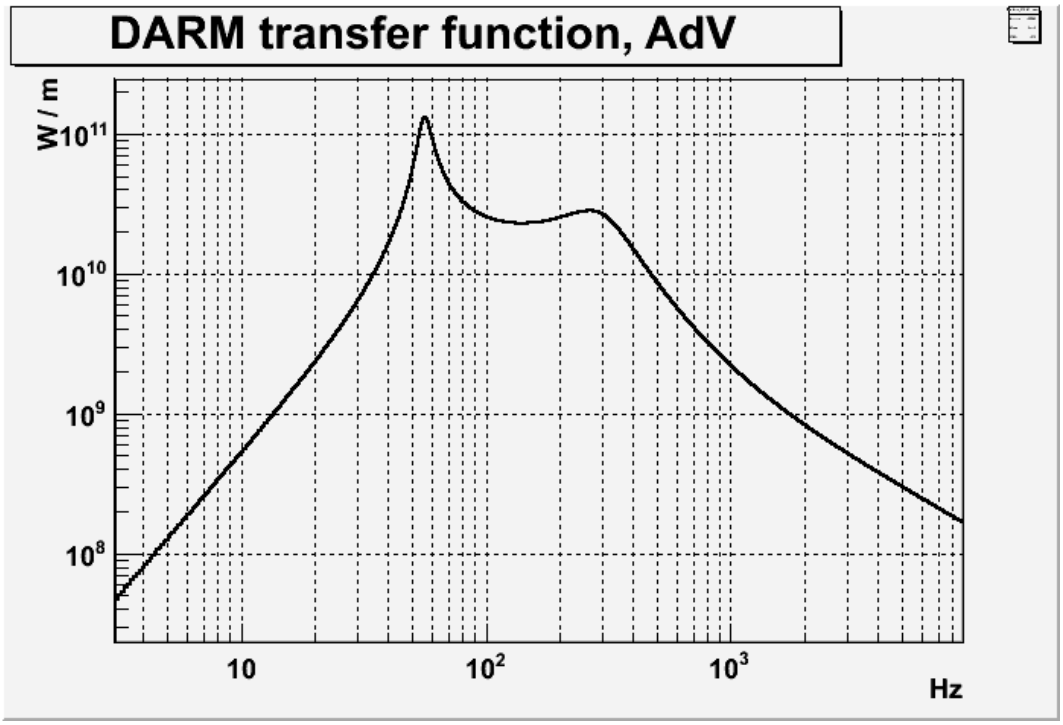

Figure 6: DARM optical response for Advanced Virgo dual recycling 125W, as simulated with Optickle [9].

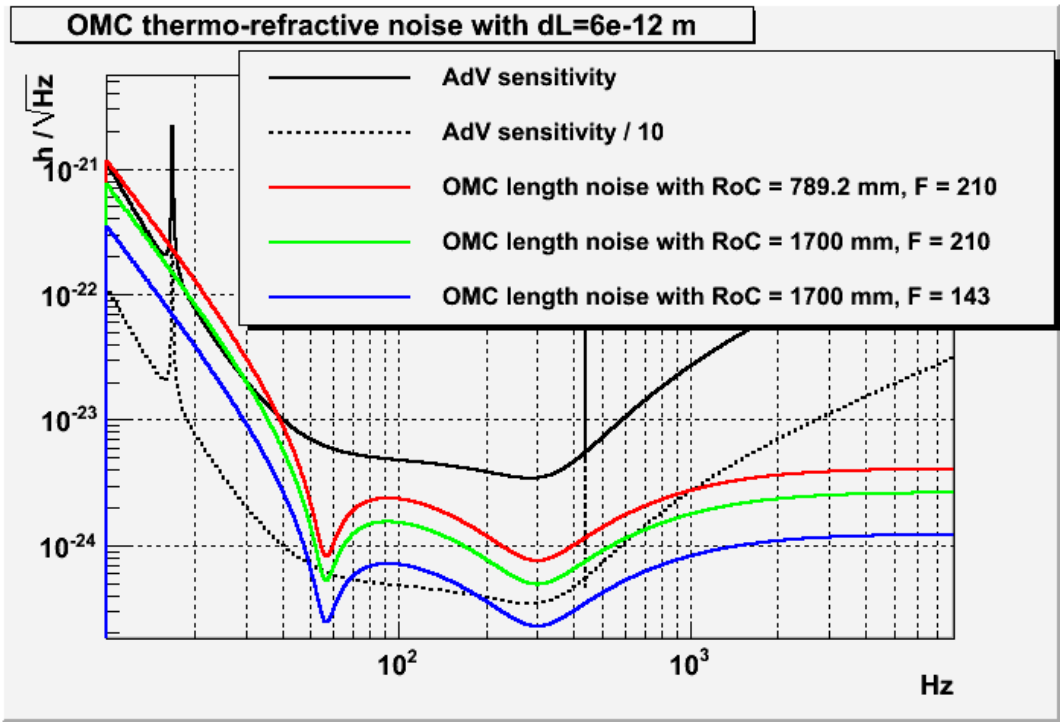

Figure 7: Projection of the OMC thermo-refractive noise compared to the Advanced Virgo sensitivity. All the noise projections shown here assume an OMC locking accuracy of 6×10^{-12} m. The red curve shows the noise projection obtained for two OMC cavities with a radius of curvature equal to 789.2 mm and a finesse equal to 210. The green curve shows the noise projection obtained when the radius of curvature (RoC) of the two cavities is increased to 1700 mm. Finally the blue curve shows the noise projection obtained when the finesse of the two cavities is lowered to 143, in addition to the increase of RoC.

following relation:

$$\delta h_{tr} = \sqrt{2}\frac{1}{TF_{DARM\rightarrow B1}}\frac{32F^2\Delta L_{omc}P_{df}}{L_{arm}\lambda^2}\delta l_{tr} \tag{7}$$

where $P_{df} \approx 80\ mW$ is the power in the carrier TEM_{00} at the dark fringe, $L_{arm} = 3000\ m$ is the arm length, and $TF_{DARM\rightarrow B1}$ refers to the optical response of the differential arm degree of freedom: this transfer function [8] was obtained by interferometer simulation [9] and is shown in Fig.6. Finally the parameter ΔL_{omc} corresponds to the OMC locking accuracy, for which an upper limit measurement was obtained with Virgo: $\Delta L_{omc} \leq 6 \times 10^{-12}\ m$. This upper limit will be used in the following to evaluate the coupling of the thermo-refractive noise to the Advanced Virgo sensitivity.

The coupling of the OMC thermo-refractive noise to the Advanced Virgo (dual recycling, 125W) sensitivity has been evaluated using Eq.7 under the conservative assumption $\Delta L_{omc} = 6 \times 10^{-12}\ m$. The results are shown in Fig. 7 for three different scenarios:

- The red curve shows the noise projection for two OMC cavities with a radius of curvature equal to 789.2 mm and a finesse equal to 210.
- The green curve shows the noise projection for two OMC cavities with a radius of curvature equal to 1700 mm and a finesse equal to 210.

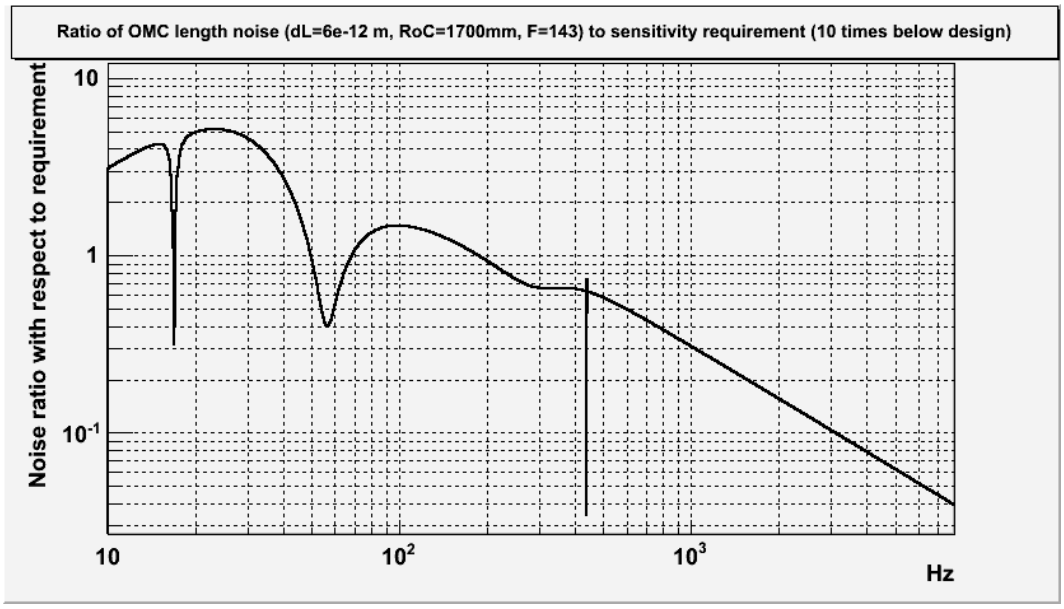

Figure 8: Ratio of the OMC thermo-refractive noise to the sensitivity requirement (which corresponds to the baseline sensitivity divided by 10), assuming a locking accuracy of 6×10^{-12} m, a radius of curvature equal to 1700 mm and a finesse equal to 143.

- The blue curve shows the noise projection for two OMC cavities with a radius of curvature equal to 1700 mm and a finesse equal to 143.

As illustrated in Fig.7 the increase of the radius of curvature from 789.2 mm to 1700 mm (which translates into an increase of the waist from 259 μm to 321 μm) allows to reduce the thermo-refractive noise by 24%. The reduction of the finesse from 210 to 143 allows to reduce further the noise coupling by a factor 2.2. Overall this optimization of the OMC parameters allows to reduce the impact of the thermo-refractive noise on the sensitivy by a factor 2.7.
The ratio of the projected OMC thermo-refractive noise to the requirement (Advanced Virgo sensitivity divided by 10) is plotted in Fig. 8, for the scenario $F = 143$ and $\rho = 1700\ mm$, and under the conservative assumption of a locking accuracy equal to $6 \times 10^{-12}\ m$. For frequencies above 50 Hz the noise projection satisfies (or nearly satisfies in the 70-200 Hz range) the requirements while in the lowest part of the detector bandwidth (10-50 Hz) the projection is above the target noise (Advanced Virgo sensitivity divided by 10) by a factor equal to or below 5.

5 Summary and conclusions

In section 2 we have shown that the optimal radius of curvature for the OMC cavities (given their nominal length $L_{geo} = 62\ mm$) is located at 1700 mm. This value allows to increase the waist to 321 μm and consequently to reduce the thermo-refractive noise by 24%, while it remains compliant with the requirements on side-band and high order modes filtering, as well as with the constraints on the beam centering within the clear aperture.
Section 3 has shown that the finesse could be lowered down to 143 while still remaining compliant with the contraints on side band and high order mode filtering for the dual recycling 125W configuration. Such a reduction of the finesse allows to further reduce the coupling of the OMC thermo-refractive noise by a factor 2.7. It must be highlighted that the requirement on the OMC filtering given by ISC [7] depends on several interferometer parameters such as the differential offset and the modulation depth of the side bands, for which some possible optimization could be investigated in order to relax the requirement on the OMC filtering. The substraction of the 6 MHz side band from the DARM error signal is also a technique that could relax further the requirements if implemented. Therefore it is likely that in the future one will find out that the finesse of the OMC cavities can be further reduced, leading to an even lower coupling of the OMC length noise.
In section 4 projections of the thermo-refractive noise for the OMC cavities have been compared to the Advanced Virgo nominal sensitivity. The residual length noise obtained with two OMC cavities presenting a radius of curvature of 1700 mm and a finesse equal to 143 is compatible with the sensitivity requirements above 50 Hz. At lower frequency a factor between 2 and 5 is missing to reach the level corresponding to the nominal sensitivity divided by a factor 10. One must emphasize that this noise projection assumes a OMC locking accuracy that corresponds to the upper limit measured with the Virgo OMC, for which the control system was

not fully optimized. Therefore a significant improvement of the locking accuracy is expected for Advanced Virgo, which should lead to a lower coupling of the OMC length noise.

References

[1] P.A. Casula, L. Digallo, R. Gouaty, F. Marion, B. Mours, L. Rolland, *Advanced Virgo Output Mode Cleaner: refinement of the design and polishing specifications*, VIR-0319A-12 (2012).

[2] R. Gouaty, P.A. Casula, L. Digallo, F. Marion, B. Mours, L. Rolland, *Advanced Virgo OMC: specifications for polisher*, VIR-0332A-12 (2012).

[3] J. Marque, G. Vajente, *Output Mode Cleaner Length Noise*, VIR-0414B-12 (2012).

[4] R. Gouaty on behalf of the DET sub-system, *DET status*, VIR-0440A-12 (2012).

[5] V.B. Braginsky, S.P. Vyatchanin, *Corner reflectors and quantum-non-demolition measurements in gravitational wave antennae*, Physics Letters A 324 (2004) 345-360.

[6] L. Di Gallo, *Maximum allowed angular errors for positioning mirrors in Advanced Virgo OMC*, VIR-0266A-12 (2012).

[7] The Virgo Collaboration, *Advanced Virgo Technical Design Report*, VIR-0128A-12 (2012).

[8] G. Vajente, *Personnal communication.*

[9] G. Vajente, *Advanced Virgo Length Sensing and Control steady state design*, VIR-0738A-11 (2011).